

Study Protocol

Study on Initial Fracture Characteristics of the Main Roof in Fully Mechanized Caving Mining of Inclined Coalbed

Hualei Zhang ¹, Yonglin Xue ^{1,*}, Yangao Li ² and Jiadi Yin ¹

¹ State Key Laboratory of Mining Response and Disaster Prevention and Control in Deep Coal Mines, Anhui University of Science and Technology, Huainan 232001, China

² Tiandi (Yulin) Mining Engineering Technology Co., Ltd., Yulin 419000, China

* Correspondence: ylxue981105@163.com; Tel.: +86-17712020991

Abstract: In view of the occurrence conditions of inclined coalbed, the deformation and failure characteristics of the main roof will affect the safe production of the working face. Therefore, the study of the deformation and failure characteristics of the main roof in the inclined coalbed has guiding significance for the control of surrounding rock. This paper takes the II1042 working face of Taoyuan Coal Mine as the research background, adopts the methods of theoretical analysis, numerical calculation, and field practice to analyze the evolutionary characteristics of the initial failure of the main roof of the working face under the background of the inclined coalbed, and explores the mechanical behavior characteristics of the working face roof during the mining of inclined coalbed. Based on the elastic thin plate theory, a mechanical model of the overlying rock roof of a large-angle coal seam is established, and the mechanical characteristics of the surrounding rock under the initial failure of the main roof under the unbalanced load are studied. The stress distribution characteristics of the lower surface are summarized, and the evolution law of the initial fracture of the main roof is summarized. According to the actual geological conditions of the II1042 working face of Taoyuan Coal Mine, the failure characteristics of the main roof and the initial breaking step distance are obtained by analysis, and the analysis results are verified by monitoring the mine pressure of each part of the target working face on site. The research results show that: ① Under the unbalanced load of the inclined coalbed, the deflection surface of the main roof of the coal seam is asymmetrical with respect to the arrangement direction of the working face, and the maximum deflection point is located at the upper middle position of the working face, namely $(a/2, 1.836 b/\pi)$, and the main roof of the working face breaks for the first time when it advances to 35 m. ② With the advancement of the working face, the two long sides of the roof break first. With the deflection and deformation of the roof, the tensile stress in the middle of the main roof reaches the tensile strength of the rock and breaks, and then the two short sides of the roof break under the action of the breaking and turning of the rock, and the upper short side will break before the lower one. ③ According to the monitoring and analysis of the rock pressure at each part of the working face, it is judged that the initial pressure step distance is between 28.2 m and 34.6 m, which is consistent with the theoretical analysis results.

Keywords: inclined coalbed; overburden failure; the first fracture; elastic thin plate theory



Citation: Zhang, H.; Xue, Y.; Li, Y.; Yin, J. Study on Initial Fracture Characteristics of the Main Roof in Fully Mechanized Caving Mining of Inclined Coalbed. *Sustainability* **2022**, *14*, 13782. <https://doi.org/10.3390/su142113782>

Academic Editor: Chaolin Zhang

Received: 9 October 2022

Accepted: 20 October 2022

Published: 24 October 2022

Publisher's Note: MDPI stays neutral with regard to jurisdictional claims in published maps and institutional affiliations.



Copyright: © 2022 by the authors. Licensee MDPI, Basel, Switzerland. This article is an open access article distributed under the terms and conditions of the Creative Commons Attribution (CC BY) license (<https://creativecommons.org/licenses/by/4.0/>).

1. Introduction

The deformation and fracture characteristics of the main roof of the inclined coalbed working face will affect the mine pressure of the working face, the anti-skid fall of the working face equipment, and the design of roadway support [1–7]. Therefore, the deformation and failure characteristics of the main roof of the inclined coalbed face are studied. It has guiding significance for control of the surrounding rock of large dip angle coal seam.

Based on the research results of near-horizontal and inclined coal seams, domestic scholars have conducted a large number of studies on the mechanical characteristics of overlying rock, deformation control, rock pressure manifestation law, the relationship

between support and surrounding rock, and the stability of support equipment in inclined coalbed working faces. Wu Yongping [8,9] studied the main roof breaking law of high-dip pseudo-subduction stope, and pointed out that due to the time sequence of stope roof breaking and caving, and the non-uniformity of gangue filling in the working face, the stope is easy to break at the spatial scale and the stope easily forms the asymmetric space on the spatial scale. Wang Jinan [10,11] took the 47,407 preliminary mining working face of Wangjiashan Coal Mine as the engineering background, established a mechanical model of the initial breakage and periodic breakage of the main roof of the inclined coalbed mining, deduced the mechanical criterion for main roof breaking, and revealed the fracture mode of the main roof of the high-dip coal seam. Zhang Yidong [12] obtained the breaking step distance of the high-dip angle working face in elevation and down-mining, respectively, by establishing the mechanical model of the roof sheet for high-dip angle and down-mining and theoretical deduction. Sun Jian [13–15] conducted theoretical research on the characteristics of the main roof stress distribution and the breaking mechanism of the working face, and obtained the theoretical calculation formula of the main roof-breaking step distance. Xie Panshi [16] studied the breaking law of the roof plate of the large inclination pseudo-inclination stope, and pointed out that the stress distribution and displacement of the roof plate of the large inclination pseudo-inclination stope were asymmetrical, and the top plate showed an asymmetrical “O-X” fracture feature. Yang Huaimin [17] monitored the displacement status of the roof plate during the mining process of the large inclination light release face, and the data analysis pointed out the relationship between the top coal of the inclined coalbed and the composite index of the top plate transport. Chai Jing [18] used the combination of BOTD and ADIC technology to study the activity law of the roof of the inclined coalbed, and found that the deformation of the roof of the inclined coalbed was asymmetrical, and the deformation of the middle and upper parts was greater than that of the lower part. Zhang Yuxiao [19] used the method of theoretical analysis to study the breaking characteristics of the roof plate of the overburden of the working face of the large inclination angle of the extra-thick coal seam, considered the filling effect of the gangue falling from the stope, and obtained the theoretical criterion of the roof breaking. Wang Shuren [20] used discrete unit software to analyze the movement law of overburden and top coal during the comprehensive mining of large inclination thick coal seam, and revealed the evolution law of stress field during the rock covering movement. Yang Zhongmin [21] took the large inclination angle of Qingshuiying Coal Mine as the research background, and used theoretical analysis and on-site monitoring methods to reveal the dynamic evolution law of large-scale mining and high-rise working face rock cover under complex engineering geological conditions. Li Junwen [22] used the method of combining FLAC numerical simulation and similar simulation tests to analyze the overburden movement of the overburden of the comprehensive mining surface of the large inclination angle thick coal seam, and divided the collapse characteristics of the overburden along the direction of the large inclination stope into four stages, and discussed in detail the movement characteristics of the overburden at each stage. Krzysztof Skrzypkowski et al. [23,24] proposed that the assessment of roof stability and the safety in long-wall space can be determined according to the basis of the index of load capacity of the roof “g” and the basis of the increased pressure in the leg of powered roof support.

In summary, many scholars have conducted much research on the deformation characteristics of the inclined coalbed roof, but the research on the fracture law of the inclined coalbed roof still needs to be deepened. In this paper, taking Taoyuan Mine II1042 working face as the engineering background, a mechanical model for the initial failure of the main roof after mining with a large dip angle is established, and the mechanical characteristics of the surrounding rock for the initial failure of the main roof under unbalanced loads are studied. The deflection of the main roof and the stress distribution characteristics of the upper and lower surfaces of the main roof during the advancing process of the working face are analyzed, and the evolution form and step distance of the initial fracture are judged.

2. Mechanical Analysis of Primary Fracture in Inclined Coalbed Mining

2.1. Mechanical Model of Primary Top Failure

According to the thin plate theory [25], the primary fracture of the main roof is regarded as an elastic thin plate with four edges clamped before the primary fracture of the main roof, and the load acting on the inclined thin plate is regarded as the resultant force of the normal component force and the tangential component force along the layer, and then the primary fracture mechanics model of the main roof is established as shown in Figure 1a. The coordinate origin is located at the boundary point of the model. The x direction is the advancing direction of the working face, the range is $(0, a)$, and the length is a . The y direction is the working face inclination, the range is $(0, b)$, and the length is b . The z direction is vertical to the top plate down.

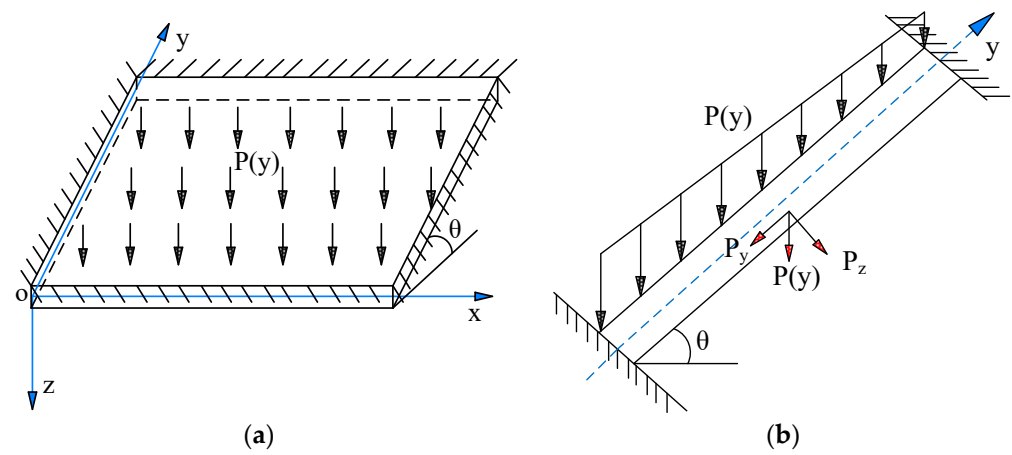


Figure 1. Mechanical model of main roof of coal seam with large dip angle.

As shown in Figure 1b, due to the different burial depths of the inclined strata, the load on the roof from the overlying strata is simplified to a load $P(y)$ that linearly increases downward along the inclination direction of the coal seam, i.e.,

$$P(y) = q_0 - ky \quad (1)$$

In the formula, q_0 is the load bearing on the main roof and bottom; k is the linear distribution coefficient of the load along the inclination direction of the main roof.

2.2. Main Roof Stress Equation of State

For a rectangular thin plate with four fixed sides, in order to reflect the linear change characteristics of the load, the deflection function of the thin plate structure before the initial collapse of the main roof is set as (x, y) [23], that is,

$$\omega = Ay \sin^2\left(\frac{\pi x}{a}\right) \sin^2\left(\frac{\pi y}{b}\right) \quad (2)$$

where A is the coefficient of the deflection function.

Equation (2) is solved using the energy method.

(1) The deformation energy formula of the plate is:

$$U = \frac{D}{2} \iint_S \left(\nabla^2 w \right)^2 + 2(1 - \mu) \left[\left(\frac{\partial^2 w}{\partial x \partial y} \right)^2 - \frac{\partial^2 w}{\partial x^2} \frac{\partial^2 w}{\partial y^2} \right] dx dy \quad (3)$$

where D is the bending stiffness of the sheet, $D = Eh^3/12(1 - \mu^2)$, E is the elastic modulus of the sheet, μ is the Poisson's ratio, h is the thickness of the main roof, and S is the overhanging area of the roof.

Because of,

$$\frac{D}{2} \iint_S 2(1-\mu) \left[\left(\frac{\partial^2 w}{\partial x \partial y} \right)^2 - \frac{\partial^2 w}{\partial x^2} \frac{\partial^2 w}{\partial y^2} \right] dx dy = D(1-\mu) \iint_S \left[\frac{\partial w}{\partial y} \left(\frac{\partial w}{\partial x} \frac{\partial^2 w}{\partial x \partial y} \right) - \frac{\partial w}{\partial x} \left(\frac{\partial w}{\partial y} \frac{\partial^2 w}{\partial y^2} \right) \right] dx dy \quad (4)$$

According to Green's formula, Equation (4) is transformed into:

$$\frac{D}{2} \iint_S 2(1-\mu) \left[\left(\frac{\partial^2 w}{\partial x \partial y} \right)^2 - \frac{\partial^2 w}{\partial x^2} \frac{\partial^2 w}{\partial y^2} \right] dx dy = D(1-\mu) \oint_L \left(\frac{\partial w}{\partial x} \frac{\partial^2 w}{\partial x \partial y} dx + \frac{\partial w}{\partial y} \frac{\partial^2 w}{\partial y^2} dy \right) \quad (5)$$

Since the boundary of the thin plate structure is clamped, combined with the boundary conditions:

$$\begin{cases} \omega|_{x=0, x=a} = 0, \omega|_{y=0, y=b} = 0 \\ \frac{\partial \omega}{\partial x}|_{x=0, x=a} = 0, \frac{\partial \omega}{\partial y}|_{y=0, y=b} = 0 \end{cases} \quad (6)$$

Then, Formula (5) is zero. The deformation energy formula of the sheet can be transformed into:

$$U = \frac{D\pi^2 A^2}{8a^3 b} \left[b^4 \left(\pi^2 - \frac{15}{8} \right) + a^4 \left(\pi^2 + \frac{15}{8} \right) + a^2 b^2 \left(\frac{2}{3} \pi^2 - \frac{1}{4} \right) \right] \quad (7)$$

(2) The lateral load work W is:

$$\begin{aligned} W &= \iint P_z \omega dx dy = \iint (q_0 - ky) \cos \theta A y \sin^2 \left(\frac{\pi x}{a} \right) \sin^2 \left(\frac{\pi y}{b} \right) dx dy \\ &= \frac{ab^2}{8} A q_0 \cos \theta - \frac{ab^3}{8} A k \cos \theta \left(\frac{2}{3} - \frac{1}{\pi^2} \right) \end{aligned} \quad (8)$$

(3) Considering only the stress analysis of the top plate under self-weight load, the strain energy V in the plate when the plate is bent under longitudinal load is:

$$V = \frac{1}{2} \iint N_y \left(\frac{\partial w}{\partial y} \right)^2 dx dy = \frac{3A^2 ab (8\pi^2 - 3)}{768} q_0 \sin \theta - \frac{3A^2 ab^2 (4\pi^2 - 9)}{512} k \sin \theta \quad (9)$$

Use the principle of minimum potential energy, $\frac{\partial \Pi}{\partial A} = \frac{\partial (U-V-W)}{\partial A} = 0$, and the following can be obtained:

$$A = \frac{32a^4 b^3 q_0 \cos \theta - 32a^4 b^4 k \cos \theta \left(\frac{2}{3} - \frac{1}{\pi^2} \right)}{\left\{ \begin{aligned} &64D\pi^2 \left[b^4 \left(\pi^2 - \frac{15}{8} \right) + a^4 \left(\pi^2 + \frac{15}{8} \right) + a^2 b^2 \left(\frac{2}{3} \pi^2 - \frac{1}{4} \right) \right] \\ &- 2a^4 b^2 (8\pi^2 - 3) q_0 \sin \theta + 3a^4 b^3 (4\pi^2 - 9) k \sin \theta \end{aligned} \right\}} \quad (10)$$

Then, the deflection curve function can be expressed as:

$$\omega = \frac{32 \left[a^4 b^3 q_0 \cos \theta - a^4 b^4 k \cos \theta \left(\frac{2}{3} - \frac{1}{\pi^2} \right) \right] y \sin^2 \left(\frac{\pi x}{a} \right) \sin^2 \left(\frac{\pi y}{b} \right)}{\left\{ \begin{aligned} &64D\pi^2 \left[b^4 \left(\pi^2 - \frac{15}{8} \right) + a^4 \left(\pi^2 + \frac{15}{8} \right) + a^2 b^2 \left(\frac{2}{3} \pi^2 - \frac{1}{4} \right) \right] \\ &- 2a^4 b^2 (8\pi^2 - 3) q_0 \sin \theta + 3a^4 b^3 (4\pi^2 - 9) k \sin \theta \end{aligned} \right\}} \quad (11)$$

Substitute the expression of the deflection function of the initial break of the main roof into the relationship between the stress and deflection function of the elastic rectangular thin plate, and obtain the principal stress expression of the initial break of the main roof with a large inclination angle:

$$\begin{cases} \sigma_1 = \frac{1}{2} [T_1 + \sqrt{T_2 + R_1}] \\ \sigma_3 = \frac{1}{2} [T_1 - \sqrt{T_2 + R_1}] \end{cases} \quad (12)$$

$$\text{where, } T_1 = -\frac{Ez}{1-\mu} \left(\frac{2\pi^2 Ay}{a^2} \sin^2\left(\frac{\pi y}{b}\right) \left[\cos^2\left(\frac{\pi x}{a}\right) - \sin^2\left(\frac{\pi x}{a}\right) \right] + \frac{2\pi^2 Ay}{b^2} \sin^2\left(\frac{\pi x}{a}\right) \left[\cos^2\left(\frac{\pi y}{b}\right) - \sin^2\left(\frac{\pi y}{b}\right) \right] + \frac{4\pi A}{b} \sin^2\left(\frac{\pi x}{a}\right) \sin\left(\frac{\pi y}{b}\right) \cos\left(\frac{\pi y}{b}\right) \right) ,$$

$$T_2 = \frac{E^2 z^2}{(1+\mu)^2} \left(\frac{2\pi^2 Ay}{a^2} \sin^2\left(\frac{\pi y}{b}\right) \left[\cos^2\left(\frac{\pi x}{a}\right) - \sin^2\left(\frac{\pi x}{a}\right) \right] - \frac{2\pi^2 Ay}{b^2} \sin^2\left(\frac{\pi x}{a}\right) \left[\cos^2\left(\frac{\pi y}{b}\right) - \sin^2\left(\frac{\pi y}{b}\right) \right] - \frac{4\pi A}{b} \sin^2\left(\frac{\pi x}{a}\right) \sin\left(\frac{\pi y}{b}\right) \cos\left(\frac{\pi y}{b}\right) \right)^2 ,$$

$$R_1 = \frac{4E^2 z^2}{(1+\mu)^2} \left(\frac{4\pi^2 Ay}{ab} \sin\left(\frac{\pi x}{a}\right) \cos\left(\frac{\pi x}{a}\right) \sin\left(\frac{\pi y}{b}\right) \cos\left(\frac{\pi y}{b}\right) + \frac{2\pi A}{a} \sin\left(\frac{\pi x}{a}\right) \cos\left(\frac{\pi x}{a}\right) \sin^2\left(\frac{\pi y}{b}\right) \right)^2 .$$

3. The Evolution Law of the Primary Failure of the Main Roof of the Inclined Coalbed

3.1. Engineering Background

Taoyuan Coal Mine is located in the northern section of the west wing of the Sunan syncline of Xusu arc structure. Taoyuan Coal Mine II1042 working face is located in the second stage of II4 mining area, which is the first working face of 10 coal seams in this mining area. The 10th coal seam of this working face belongs to the Permian Shanxi Formation. The thickness of the 10th coal seam is 3.2–4.2 m, and there is a layer of intercalated gangue, which is 0–0.23 m thick. The average dip angle of the coal seam is 38°. The roof of the coal seam is composed of rocks such as mudstone and fine sandstone, and the bottom plate is mudstone. The II1042 working face of Taoyuan Mine adopts a single-strike longwall comprehensive mechanized coal mining method, and uses hydraulic support to timely support the exposed roof to reduce the occurrence of roof fall accidents. The histogram of the coal seam at the working face is shown in Figure 2 below.

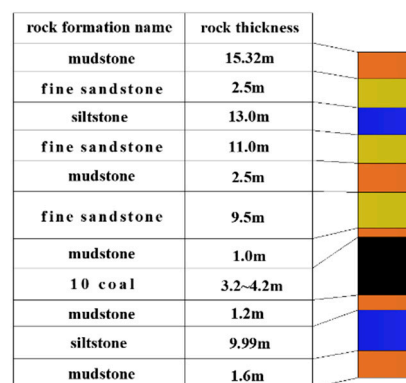


Figure 2. Bar chart of rock strata.

In view of this engineering background, the roof and coal wall management is difficult, the propulsion speed is slow, and the hydraulic support is seriously damaged, according to the mechanical analysis of the initial fracture of the main roof during the mining process of the inclined coalbed in the previous section, combined with the overburden stratum parameters of the II1042 working face of Taoyuan Mine, taking $h = 9.5$ m, $E = 13$ GPa, $b = 160$ m, $\theta = 350$, $q = 0.6$ MPa, $\mu = 0.25$, $k = 0.001$, so we must analyze the main roof deflection, stress distribution, and initial breaking step distance during the advancing process of the working face.

3.2. Fundamental Top First Break Deflection Parameter Analysis

Combining Equation (10) with the parameters of the overlying strata, the deflection surface of the main roof at different advancing distances of the working face is drawn, as shown in Figure 3.

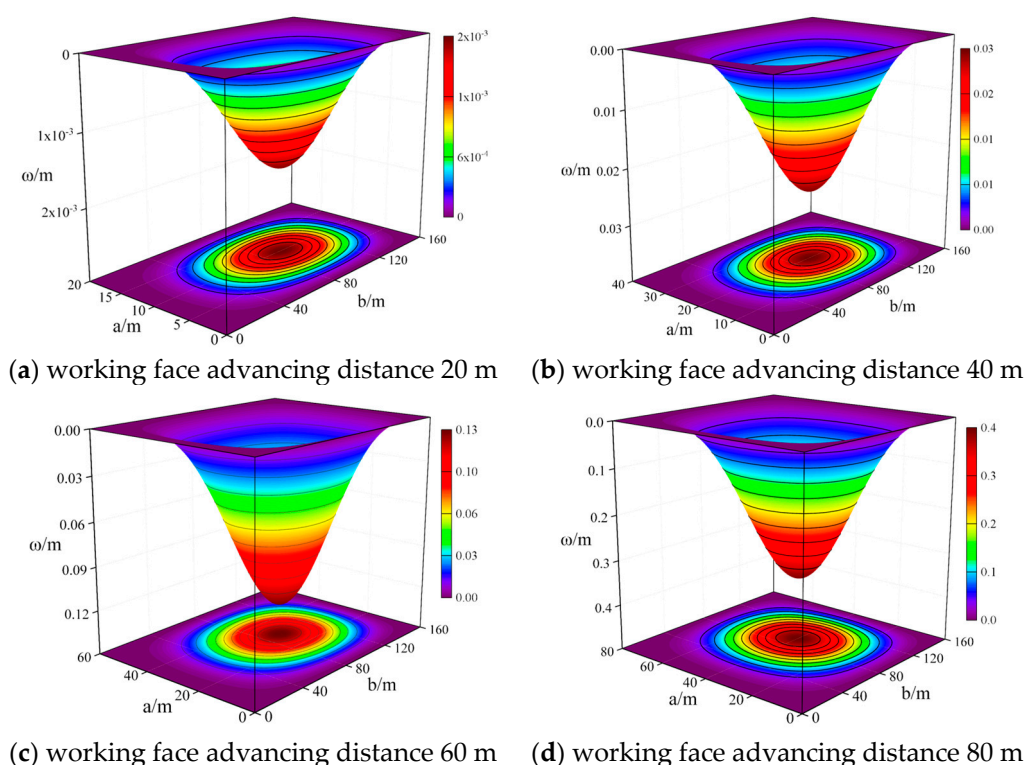


Figure 3. Main roof deflection diagram.

It can be seen from Figure 3 that with the continuous advancement of the working face, the deflection of the main roof continues to increase. Under the joint action of uneven loads, the deflection surface of the main roof of the inclined coalbed is symmetrical about the direction of the working face, and asymmetrical in the direction of the working face arrangement. The maximum deflection point is located in the upper middle of the working face, showing the difference in the deformation characteristics of the horizontal apical slate layer.

Since the overburden load on the main roof is linearly distributed along the y -axis direction, the main roof deflection curve is asymmetric, the deflection surface is symmetrically distributed in the direction of the working face, and asymmetrically distributed in the advancing direction of the working face. It can be seen from Figure 3 that the maximum deflection position of the main roof lies on the line $x = a/2$. At this time, $\partial w / \partial x = 0$, the first partial derivative of the main roof deflection function to y can be obtained, that is, the coordinates of the maximum deflection point.

Perform a partial derivative of y on the deflection function, substitute $x = a/2$, and get:

$$A \sin\left(\frac{\pi y}{b}\right) \left(\frac{2\pi y}{b} \cos\left(\frac{\pi y}{b}\right) + \sin\left(\frac{\pi y}{b}\right) \right) = 0 \quad (13)$$

According to the asymmetry of the deflection in the y direction, it can be seen that the deflection maximum point is $y \neq b/2$, so Equation (12) can be converted to:

$$\frac{2\pi y}{b} \cos\left(\frac{\pi y}{b}\right) + \sin\left(\frac{\pi y}{b}\right) = 0 \quad (14)$$

The image method is used to solve the function zero-point problem, and then the coordinates of the maximum deflection point of the main roof first break are $(a/2, 1.836 b/\pi)$.

3.3. Analysis of Stress Distribution Parameters of Primary Top Breaking

In order to investigate the force characteristics of the main roof and then analyze the initial breaking distance of the main roof, according to the theoretical analysis results and

the parameters of the overburden layer on the working face of Taoyuan Mine II.1042, the contour plot of the maximum principal stress on the upper and lower surfaces of the main roof is drawn by Matlab.

From Figures 4 and 5, it can be seen that the maximum principal stress of the upper and lower surfaces of the main roof is symmetrically distributed in the x direction and asymmetrically distributed in the y direction. The maximum value of the maximum principal stress occurs at the upper position of the midpoint in the y direction. The parametric analysis shows that the maximum principal stress reaches the maximum at $(a/2, 1.836 b/\pi)$.

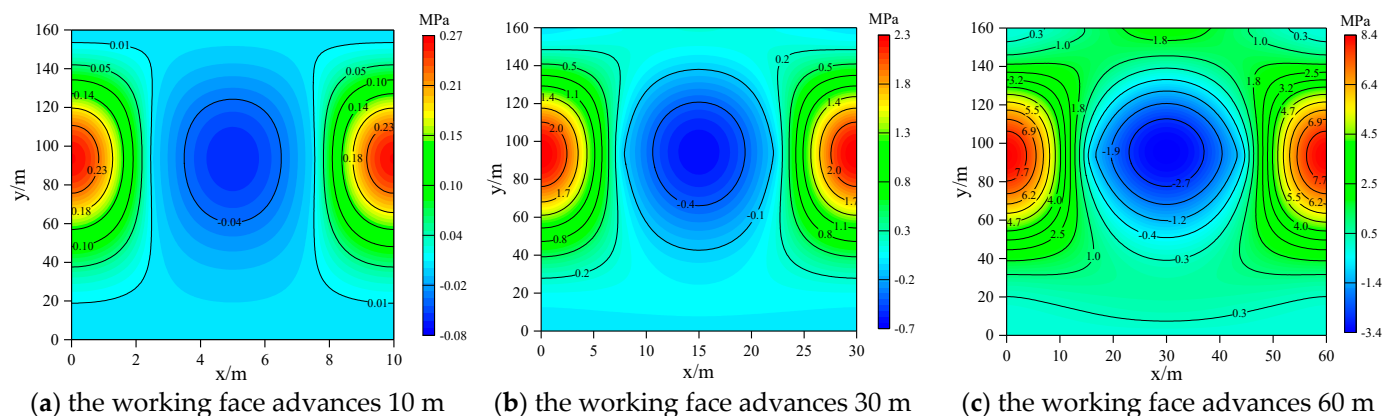


Figure 4. Contours of the maximum principal stress distribution of the main roof surface.

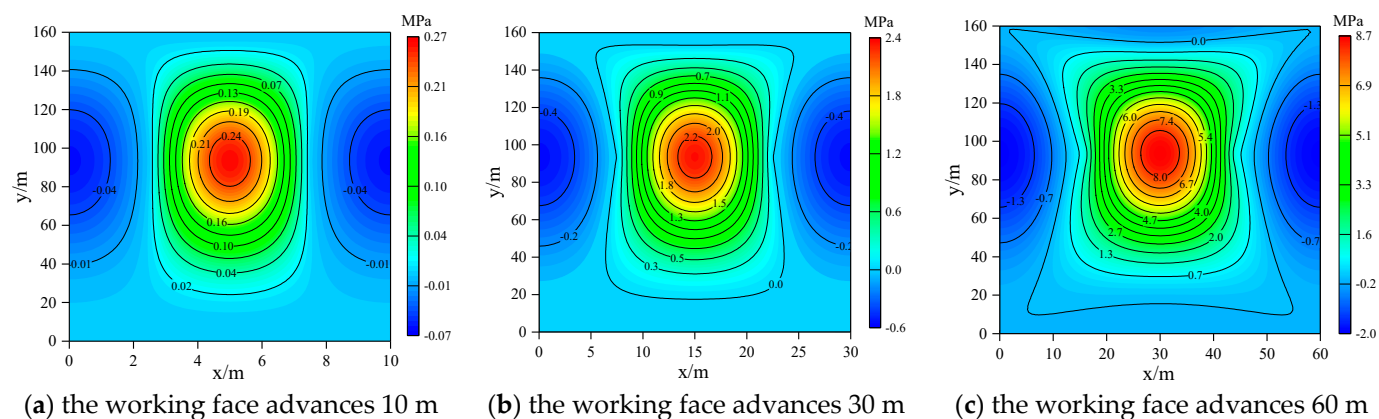


Figure 5. Contours of the maximum principal stress distribution of the basic sub-top surface.

As seen from Figure 4, the maximum principal stress of the upper surface of the main roof appears in the center of the fundamental top long side, showing a semi-elliptical distribution. As the working face advances, the maximum principal stress increases from 0.27 MPa to 8.4 MPa. The contours of the maximum principal stress exhibit an elliptical distribution at the geometric center of the main roof. It is a negative value, indicating that the main roof surface is stretched on both sides and pressurized in the middle. The maximum principal stress of the two short sides of the main roof gradually decreases from the upper position to the lower position. With the advancement of the working face, the maximum principal stress at the center of the upper short side increases from 0.01 MPa to 1.8 MPa, which is much smaller than the maximum principal stress of the long side. According to the distribution characteristics of the maximum principal stress on the upper surface of the main roof, the breaking sequence of the upper surface of the main roof is from the two long sides to the upper short side and then to the lower short side.

As seen from Figure 5, the maximum principal stress on the lower surface of the basic top appears at the geometric center of the main roof, showing an elliptical distribution. As

the working face advances, the maximum value of the maximum principal stress increases from 0.27 MPa to 8.7 MPa. The contour lines of the maximum principal stress show a semi-elliptical distribution on the long sides of the main roof and are negative, indicating that the lower surface of the main roof is in a state of compression on four sides and tension in the middle. With the continuous advancement of the working face, the tension area gradually transforms from an ellipse to an “X-shape”.

3.4. Main Roof First Break Step Distance Analysis

The strength characteristics of rock are σ compression $>$ σ shear $>$ σ tension, so the failure mode of the main roof during the advancing process of the working face is mainly tensile failure. According to the maximum tensile stress criterion, when the maximum principal stress σ_1 in the rock is greater than the maximum tensile strength of the rock, the rock will be damaged and unstable. According to the analysis of the mechanical parameters of the initial failure of the main roof in the previous section, it can be inferred that the initial failure criterion of the main roof is:

$$\sigma_1|_{x=(0,a/2),y=1.836b/\pi} = \frac{1}{2}[T_1 + \sqrt{T_2 + R_1}] > [\sigma_t] \quad (15)$$

According to the relevant geological parameters of the II1042 working face of Taoyuan Mine, the tensile strength of the rock of the main roof is taken as 2.4 MPa, and the relationship between the maximum principal stress of the main roof and the advancing distance of the working face is obtained by using Matlab mathematical software and origin drawing software, as shown in Figure 6. It can be calculated that the main roof breaks for the first time when the working face advances 35 m.

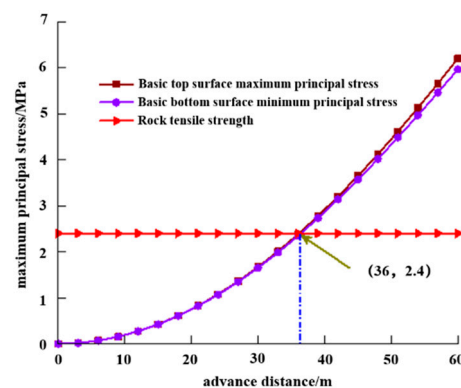


Figure 6. Maximum principal stress curve of the main roof and lower surfaces.

4. Simulation Analysis of Stress Variation in High Dip Coal Seam Working Face

4.1. Numerical Model Building

The FLAC3D software is used to create a 3D model of the recovery of the inclined coalbed face, as shown in Figure 7. The width of the working face is 165 m, the thickness of the coal seam is 4.2 m, the horizontal width of the coal body on both sides of the working face is 80 m, and the length in the advancing direction of the working face is 250 m. The upper surface of the model is a free face, and displacement constraints are applied to the bottom surface of the model and the remaining four sides. The effect of the upper rock layer of the model on the model can be approximated as a uniform load q , that is, the self-weight of the overlying rock layer is $q = \gamma H'$, and H' is the thickness of the overlying rock. The damage of material adopts Mohr–Coulomb criterion, and the mined-out area is processed by the null model. The physical and mechanical properties of the coal rock formation in the model are shown in Table 1.

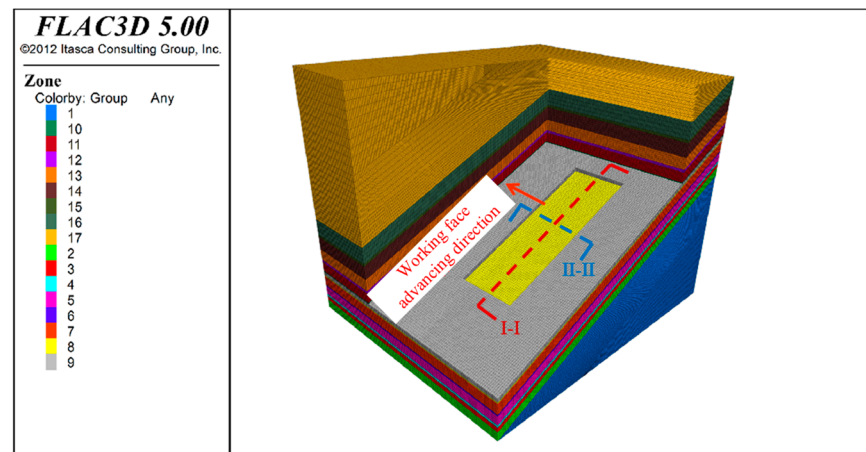


Figure 7. Numerical calculation model.

Table 1. Physical and mechanical parameters of each rock layer.

Rock Stratum	Shear Elasticity/GPa	Bulk Modulus/GPa	Cohesion/GPa	Tensile Strength/MPa	Density/kg/m ³	Frictional Angle/°
aleuvite	2.4	4.5	3.2	2.4	2500	40
argillite	1.6	3	2.2	1.2	2500	30
packsand	9	5.8	4.2	2.8	2800	34
10 coal	1.2	2	1.8	0.9	1600	23

4.2. Analysis of Support Stress in Stope of Large Dip Angle Coal Seam

It can be seen from the distribution of concentrated stress on the lateral coal wall of the inclined coalbed working face (Figure 8) that for the upper or lower end of the inclined coalbed working face, the stress increases with the increase in the advancing step. The stress concentration range of the coal wall at the lower end of the working face is smaller than that at the upper end. The concentrated stress of the coal wall at the lower end of the initial mining face is higher than that at the upper end. With the advancement of the working face, the concentrated stress of the two gradually approaches.

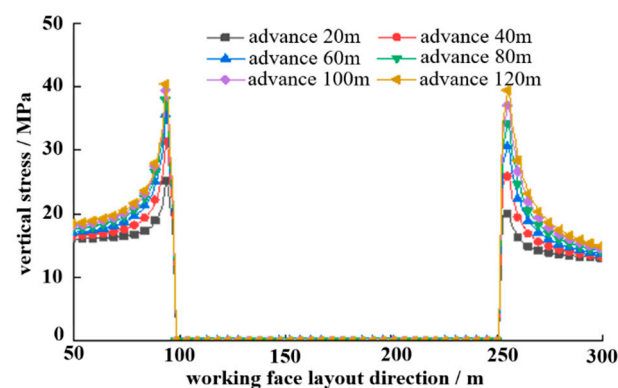


Figure 8. Distribution of lateral coal wall concentration on the working face of the coal seam.

According to the distribution of the support pressure in front of the working face of the inclined coalbed (Figure 9), it can be seen that when the coal seam advances from the vicinity of the incision, the peak value and concentration range of stress are both small. With the continuous advancement of the working face, the advance support pressure continues to increase, and it is transferred to the solid coal in front of the working face. The stress concentration coefficient in front of the working face gradually increases and tends to be

stable. When the working face is advanced by 40 m, the stress concentration coefficient increases greatly. When the working face is advanced to 120 m, the rock mass that has collapsed before the goaf is gradually compacted, the peak value of the support pressure is about 42 MPa, and the stress concentration coefficient basically tends to be stable.

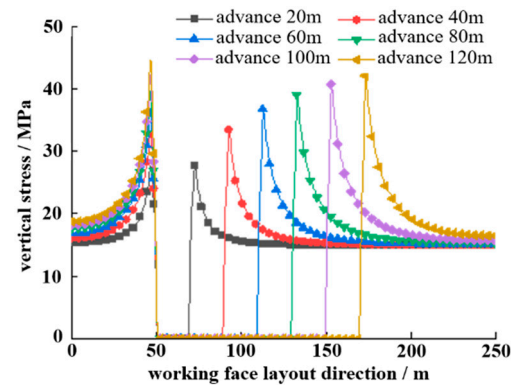


Figure 9. Distribution of support pressure in front of the work.

4.3. Comparative Analysis of Stress at Different Positions of Working Face Inclination

When the working face advances by 40 m, 80 m, and 120 m, we can compare the stress evolution law of its lower part, middle lower part, middle part, middle upper part, and upper part, and draw the maximum concentrated stress curve, as shown in Figure 10. It can be seen from the figure that with the advancement of the working face, the maximum concentrated stress in front of the working face shows an increasing trend. The peak concentrated stress in the middle, upper middle, and lower middle is larger than that in the upper and lower parts by 4.3% to 6.6%.

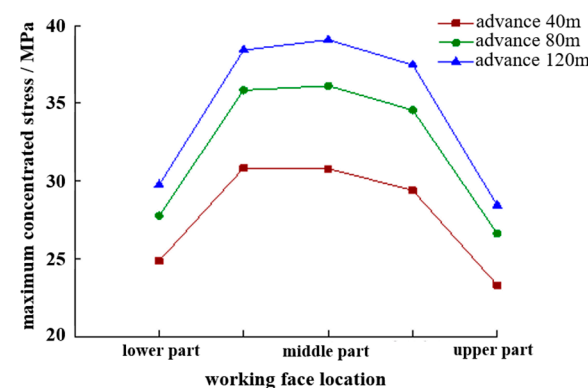


Figure 10. Maximum concentrated stress curves at different propulsion distances.

When the working face is advanced by 40 m, the maximum concentrated stress of the upper and lower parts is 24.3% and 19.2% smaller than that of the middle part. When the working face is advanced by 80 m, the maximum concentrated stress of the upper and lower parts is, respectively, 26.3% and 23.1% smaller than that of the middle part. When the working face is advanced by 120 m, the maximum concentrated stress in the upper and lower parts is 27.2% and 23.8% smaller than that in the middle. The results show that as the working face advances, the difference between the peak concentration of stress in the middle and the two ends tends to increase, and the stress concentration in the middle becomes more obvious.

5. Analysis on the Appearance of Rock Pressure at the First Fracture of the Main Roof

The mine pressure monitoring of the II1042 working face in Taoyuan Mine was carried out, and the time series characteristics of the mine pressure at the working face during

the initial roof fracture were mastered. The monitoring stations of the stent resistance are arranged from bottom to top, and continuously monitor the changes of stent resistance at four positions below the working face, lower middle, upper middle, and upper.

Figure 11 shows the change in the support resistance with the advancement of the working face. The working face is pressed from the middle, upper middle, and upper parts for the first time, and finally, the order of the middle lower part and the lower part is carried out in turn. The upper and middle parts are pressed first, and the deflection deformation of the overlying rock in the middle and upper parts of the working face is the largest and breaks first. Comprehensive analysis of the working face pressure time and advancing distance shows that the pressure step distance at different positions of the working face is between 28.2 m and 34.6 m, and the average step distance is 31.6 m. There are differences in the stepping distance at different positions of the working face, and the average stepping distance in the middle and upper parts is the smallest. The working resistance of the hydraulic support in the lower and middle and lower parts of the working face is greater than that in the middle, upper middle, and upper parts. This is mainly because the top plate first breaks in the middle and upper parts. After the top plate is broken and rotated, the stress is transferred to the lower part. The load acting on the lower part and the middle and lower part of the roof plate is relatively large. The working resistance of the regional hydraulic support is high.

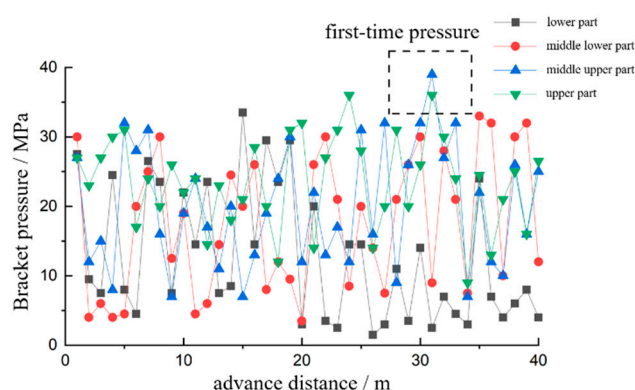


Figure 11. Variation of support resistance.

6. Conclusions

(1) Using the elastic thin plate theory, the mechanical model of the fracture of the inclined coalbed roof was established, and the deflection equation of the roof under the unbalanced load of the high-dip-angle working face was deduced. Through the parameter analysis, it is concluded that the coordinates of the maximum deflection point of the initial fracture of the main roof is $(a/2, 1.836 b/\pi)$, and the initial fracture of the main roof occurs when the working face advances to 35 m.

(2) According to the analysis results of the initial fracture of the main roof, the two long sides of the main roof are broken first. With the deflection and deformation of the roof, the tensile stress in the middle reaches the tensile strength of the rock, and the fracture occurs. During the breaking and rotation process of the roof, the two short sides are broken, and the upper short side will break before the lower one.

(3) By establishing the FLAC3D numerical model, the stress distribution state of the surrounding rock when the working face advances at different distances is analyzed. The results show that the concentrated stress of the coal wall of the working face increases gradually with the advancement of the working face, and the peak value of the stress concentration gradually tends to stabilize when the working face advances to 60 m. With the advancement of the working face, the concentrated stress in front of the working face tends to be unevenly distributed in the rock formation, and the difference between the peak concentrated stress in the middle and the peaks at both ends tends to increase, and the stress concentration in the middle area is more obvious.

(4) According to the analysis of the pressing time and advancing distance of the working face, the initial pressure step distance at different positions of the working face is between 28.2 m and 34.6 m, and the average step distance is 31.6 m. The order of pressure applied to each part is different, the middle and upper part and the middle part are pressed first, and the deflection deformation of the overlying rock in the middle and upper part of the working face is the largest.

Author Contributions: Conceptualization, H.Z. and Y.X.; methodology, J.Y.; software, Y.L.; validation, H.Z., Y.X. and Y.L.; resources, H.Z.; data curation, H.Z. and Y.X.; writing—original draft preparation, Y.X.; writing—review and editing, H.Z. All authors have read and agreed to the published version of the manuscript.

Funding: This work is supported by the University of Synergy Innovation Program of Anhui Province No. GXXT-2019-029.

Institutional Review Board Statement: Not applicable.

Informed Consent Statement: Not applicable.

Data Availability Statement: Not applicable.

Conflicts of Interest: The authors declare no conflict of interest.

References

- Kang, X.; Yang, S.; Zhan, P.; Li, L. Simulation Study of the Roof Fracture Pattern of a Horizontal Sublevel Caving in a Steeply Inclined Thick Coal Seam. *Adv. Civ. Eng.* **2020**, *2020*, 8370634. [\[CrossRef\]](#)
- Wang, H.; Qin, Y.; Wang, H.; Chen, Y.; Liu, X. Process of overburden failure in steeply inclined multi-seam mining: Insights from physical modelling. *R. Soc. Open Sci.* **2021**, *8*, 210275. [\[CrossRef\]](#) [\[PubMed\]](#)
- Li, X.; Wang, Z.; Zhang, J. Stability of roof structure and its control in steeply inclined coal seams. *Int. J. Min. Sci. Technol.* **2017**, *27*, 359–364. [\[CrossRef\]](#)
- Çelik, A.; Özçelik, Y. Investigation of the efficiency of longwall top coal caving method applied by forming a face in horizontal thickness of the seam in steeply inclined thick coal seams by using a physical model. *Int. J. Rock Mech. Min. Sci.* **2021**, *148*, 104917. [\[CrossRef\]](#)
- Wang, H.; Wu, Y.; Jiao, J.; Cao, P. Stability Mechanism and Control Technology for Fully Mechanized Caving Mining of Steeply Inclined Extra-Thick Seams with Variable Angles. *Min. Metall. Explor.* **2021**, *38*, 1047–1057.
- Zhang, H.; Hu, G.; Zhao, G. Research on the Movement Law of Roof Structure in Large-Inclined Coal Seam Working Face: A Case Study in Liu.Pan.Shui. Mining Area. *Shock Vib.* **2022**, *2022*, 6328851. [\[CrossRef\]](#)
- Wang, S.; Dou, L.; Mu, Z.; Cao, J.; Li, X. Study on Roof Breakage-Induced Roadway Coal Burst in an Extrathick Steeply Inclined Coal Seam. *Shock. Vib.* **2019**, *2019*, 2969483. [\[CrossRef\]](#)
- Wu, Y.; Liu, W.; Xie, P.; Tian, S. Stress Evolution and Roof Breaking Characteristics of Surrounding Rock in Oblique Longwall Mining Area of Steeply Dipping Seam. *J. Coal* **2020**, *51*, 222–227.
- Wu, Y.; Wang, H.; Xie, P. Analysis of surrounding rock macro stress arch-shell of longwall face in steeply dipping seam mining. *J. Coal* **2012**, *37*, 559–564.
- Wang, J.; Zhang, J.; Gao, X.; Wen, J.D.; Gu, Y.D. Fracture mode and evolution of main roof stratum above longwall fully mechanized top coal caving in steeply inclined thick coal seam (I)—Initial fracture. *J. Coal Sci.* **2015**, *40*, 1353–1360.
- Wang, J.; Zhang, J.; Gao, X.; Wen, J.D.; Gu, Y.D. Fracture mode and evolution of main roof stratum above fully mechanized top coal caving longwall coalface in steeply inclined thick coal seam (II): Periodic fracture. *J. Coal* **2015**, *40*, 1737–1745.
- Zhang, Y.D.; Cheng, J.Y.; Wang, X.X.; Feng, Z.J.; Ji, M. Thin Plate Model Analysis on Roof Break of Up-Dip or Down-Dip Mining Stope. *Chin. J. Min. Saf. Eng.* **2010**, *27*, 487–493.
- Sun, J.; Liu, X.; Ren, T. Overburden stability of an inclined backfill stope in the context of the nonlinear elastic mechanical properties of the backfill body. *Environ. Earth Sci.* **2019**, *78*, 719. [\[CrossRef\]](#)
- Sun, J.; Wang, L.; Zhao, G. Failure Characteristics and Confined Permeability of an Inclined Coal Seam Floor in Fluid-Solid Coupling. *Adv. Civ. Eng.* **2018**, *2018*, 2356390. [\[CrossRef\]](#)
- Jian, S.; Yang, H. Mechanical properties of fixed rectangular thin plates under uniform distribution and hydrostatic pressure. *Appl. Mech.* **2015**, *32*, 908–914; 1096–1097.
- Xie, P.; Tian, S.; Duan, J. Experimental study on the movement law of roof in pitching oblique mining area of steeply dipping seam. *J. Coal* **2019**, *44*, 2974–2982.
- Yang, H.; Cui, J.; Liu, H. Quantitative analysis of roof migration of top coal in light caving face of large dip angle coal seam. *Coal Eng.* **2003**, *4*, 41–42.
- Chai, J.; Du, W.G.; Zhang, D.D.; Lei, W. Study on roof activity law in steeply inclined seams based on BOTDA sensing technology. *Chin. J. Rock Mech. Eng.* **2019**, *38*, 1809–1818.

19. Zhang, Y.; Wang, K. Roof Broken Features at Fully Mechanized Caving Mining Stope in Steep Inclined and Specially Thick Seam. *Coal Mine Saf.* **2014**, *7*, 187–191.
20. Wang, S.; Wang, J.; Dai, Y. Discrete Element Analysis on Movement Law and Failure Mechanism of Top Coal in Fully-mechanized Caving Mining of Thick Coal Seam with Large Dip Angle. *J. Univ. Sci. Technol. Beijing* **2005**, *1*, 5–8.
21. Yang, Z.; Zhang, J.; Lai, X.; Lv, Z. Localized character of strata movement for complicated super-thick water-rich coal seam with large mining height. *J. Coal* **2010**, *35*, 1868–1872.
22. Cheng, W.; Li, J. Stope wall rock activity law of long-wall full-mechanized caving mining on strike of steep dipping seam. *China Min. Ind.* **2009**, *5*, 56–58.
23. Skrzypkowski, K.; Korzeniowski, W.; Duc, T.N. Choice of powered roof support FAZOS-15/31-POz for Vang Danh hard coal mine. *Inżynieria Miner.* **2019**, *21*, 175–182. [[CrossRef](#)]
24. Łukasz, H.; Dariusz, J.; Krzyszto, S. Powered Roof Support—Rock Strata Interactions on the Example of an Automated Coal Plough System. *Stud. Geotech. Mech.* **2018**, *40*, 46–55. [[CrossRef](#)]
25. Wu, G.; Chen, W.; Jia, S.; Tan, X.; Zheng, P.; Tian, H.; Rong, C. Deformation characteristics of a roadway in steeply inclined formations and its improved support. *Int. J. Rock Mech. Min. Sci.* **2020**, *130*, 104324. [[CrossRef](#)]